Journal of ELECTRICAL ENGINEERING, VOL 72(2021), NO6, 407–412

sciendo

PAPERS

A wideband dual-circularly polarized traveling wave antenna array

Jia-Lin Li[1,5] Long-Jie Wang[1], Jin Liu[1], Kexin Song[2], Ye Jin[2], Baidenger Agyekum Twumasi[3,4]

A dual-circularly polarized traveling wave antenna based on linear polarization array with wideband response is proposed. The circular polarization is realized by the sequential rotation arrangement of four linear polarization elements and series feeding with a phase difference 90°. Rotating four of such subarrays sequentially with a phase difference of 90° not only broadens the axial ratio (AR) bandwidth but also corrects the pattern beam deflection. Left-handed circular polarization (LHCP) and right-handed circular polarization (RHCP) are respectively achieved by exciting two different ports. The measured impedance bandwidth of the developed antenna array is 27.5 %. The 3-dB AR bandwidths of RHCP and LHCP are respectively 20.7 % and 22.4 % with the peak gains of about 8.7 and 8.3 dBic.

K e y w o r d s: dual-circular polarization, 90°phase difference, series-feeding, traveling wave, rectangular patch

1 Introduction

In todays wireless communications, circularly polarized (CP) antennas can reduce multipath effects and avoid polarization alignment between transmitter and receiver. Therefore, circularly polarized antennas are widely used in wireless systems, such as satellite communication systems and global positioning systems.

Sequential rotation is widely used to extend the axial ratio (AR) bandwidth of CP antennas. To now, different methods combined with sequential rotation techniques are studied to construct a CP array [1]-[4]. On the other hand, it is known the dual-CP antennas can increase channel capacity and miniaturize wireless communication systems, hence dual-CP antennas are one of hot topics. Based on the interlaced sequential rotation technique, a loop-fed dual-CP antenna is reported in [5]. A U-shaped slot antenna realizes broadband dual circular polarization in [6]. In [7], a SIW horn antenna is proposed, where the desired phase shift as a result of the difference of the guided wavelength of the two orthogonal modes generates a circularly polarized wave. A novel traveling wave antenna using a square microstrip patch with a chamfered corner can achieve dual circular polarization [8]. Dual-CP antennas using sequential rotation and series feeding are of typical wideband responses [9–11]. In general, the AR bandwidth and impedance bandwidth are basic challenges for wideband dual-CP antennas and antenna arrays.

In this paper, a low-cost dual-CP traveling wave antenna array with wideband characteristics is proposed. The circular polarization is realized by the sequential rotation arrangement of four linear polarization elements [12]. Based on the traveling wave operation mechanism, series fed is utilized to broaden the impedance bandwidth. The rotating four of such subarrays forms a 4×4 array with widened AR bandwidth. The gain response of the subarray and the signal transmission mechanism of the 4×4 array are analyzed.

2 Studying the subarray based on linearly polarized element

Figure 1 shows the configuration of the proposed 2×2 subarray that is realized on a microwave substrate with $\varepsilon_r = 2.2$ and thickness $h = 0.5$ mm. It consists of four half-wavelength rectangular patches and three quarter-wavelength microstrip transmission lines. Each patch generates linearly polarized wave. With the square loop guiding based traveling wave on each element one after another, a circularly polarized wave can be generated, where port A corresponds to the LHCP, port B corresponds to the RHCP.

The phase difference between adjacent elements is represented by $\Delta\varphi$. The electrical length of the element is $\lambda_g/2$, and the electrical length of the transmission line is $\lambda_g/4$. However, the electrical length changes with frequency, so $\Delta\varphi$ can be expressed as

$$\Delta\varphi = (180^\circ + 90^\circ)\frac{f}{f_0}. \tag{1}$$

[1] School of Physics, University of Electronic Science and Technology of China, Chengdu 611731, China, [2] Shanghai Aerospace Electronic Technology Institute, shanghai 201109, China, [3] School of Resources and Environment, University of Electronic Science and Technology of China, Chengdu 611731, China, [4] Electrical/Electronic Engineering Department, Ho Technical University, Ho, Ghana, jialinli@uestc.edu.cn, sskkxx@263.net; jyisrobin@126.com, btwumasi@htu.edu.gh, [5] State Key Laboratory of Millimeter Waves, Southeast University, Nanjing 210096, China

https://doi.org/10.2478/jee-2021-0058, Print (till 2015) ISSN 1335-3632, On-line ISSN 1339-309X

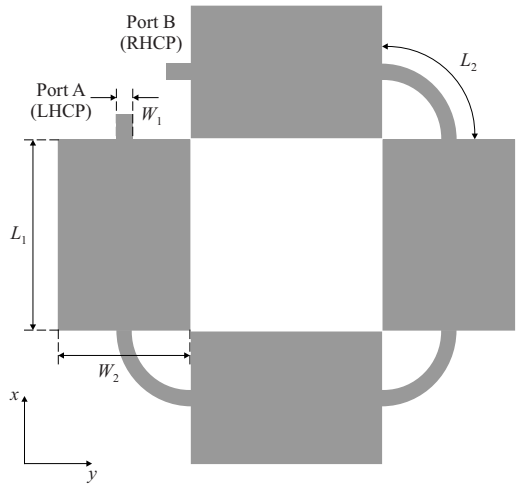

Fig. 1. Structure of the proposed 2×2 subarray (parameters $L_1 = 17.4$ mm, $L_2 = 9.5$ mm, $W_1 = 1.5$ mm, $W_2 = 12$ mm)

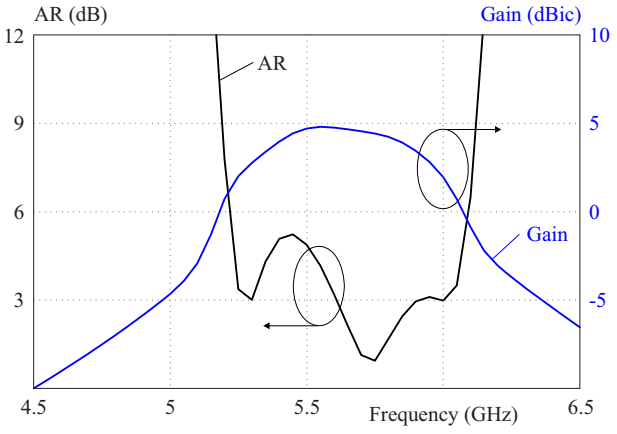

Fig. 2. Simulated gain and AR of the 2×2 subarray

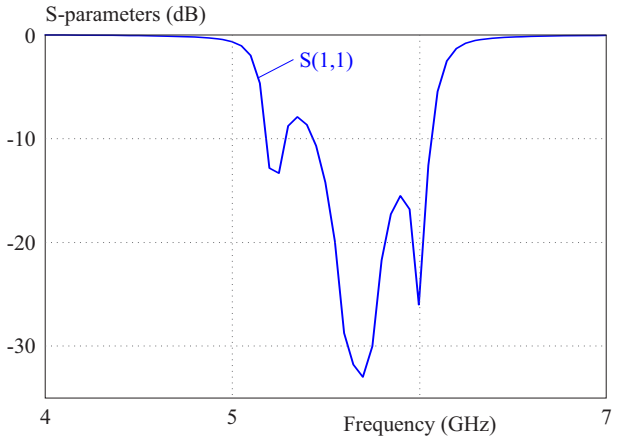

Fig. 3. Simulated S-parameters of the 2×2 subarray

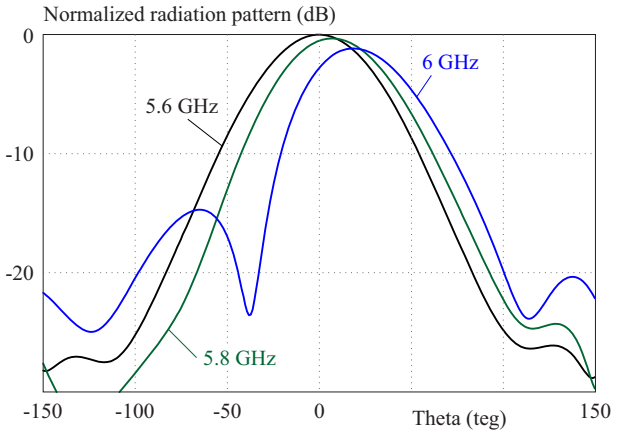

Fig. 4. Simulated normalized radiation pattern of the 2×2 subarray at different frequencies

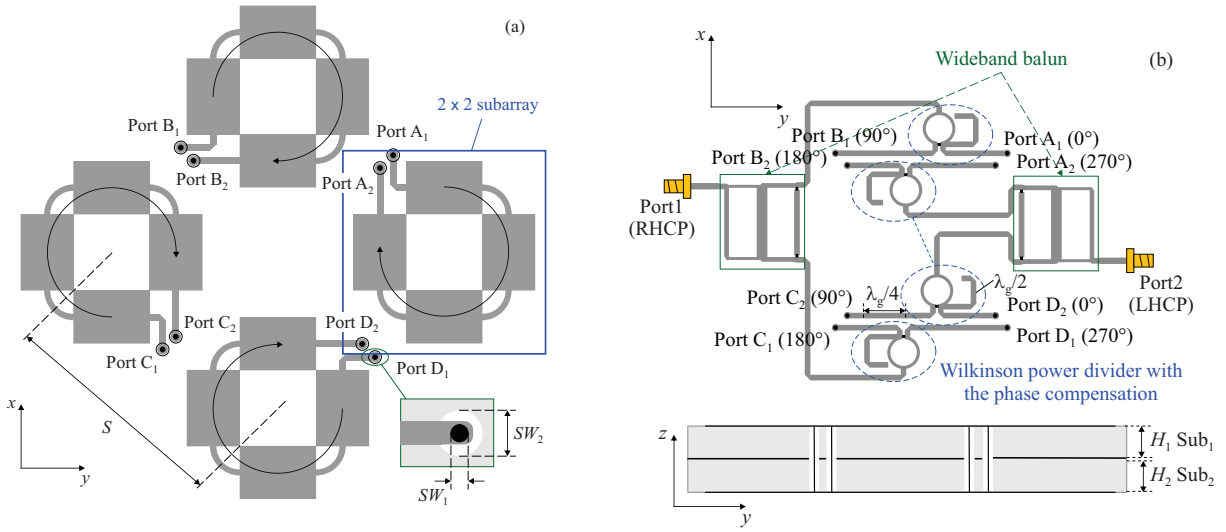

Fig. 5. Configuration of the traveling wave antenna array: (a) – radiation patches on the top layer, where the green arrows denote the signal flow, (b) – Dual-port feeding network at the bottom layer

The simulated gain and AR of the antenna subarray are shown in Fig. 2. The AR bandwidth for AR < 3 dB is 5.3 %, covering from 5.61 to 5.92 GHz. The small AR bandwidth is due to the energy imbalance among each patch and the phase imbalance of the transmission lines between patches at different frequencies. This also yields

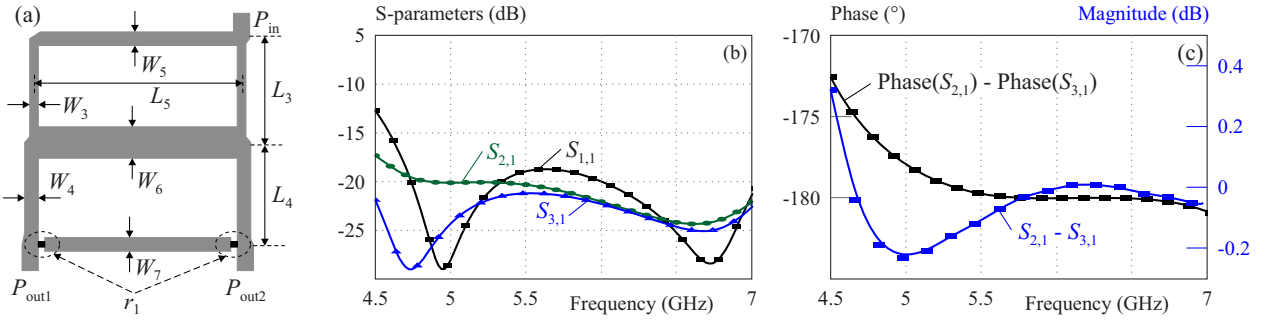

Fig. 6. Configuration of the branch-line balun: (a) – optimal parameters (in mm): $L_3 = 10$, $L_4 = 9.5$, $L_5 = 19$, $W_3 = 0.8$, $W_4 = 1.25$, $W_5 = 1.25$, $W_6 = 2.9$, $W_7 = 1.25$, (b) – simulated S-performance, and (c) – phase and magnitude imbalances of the balun

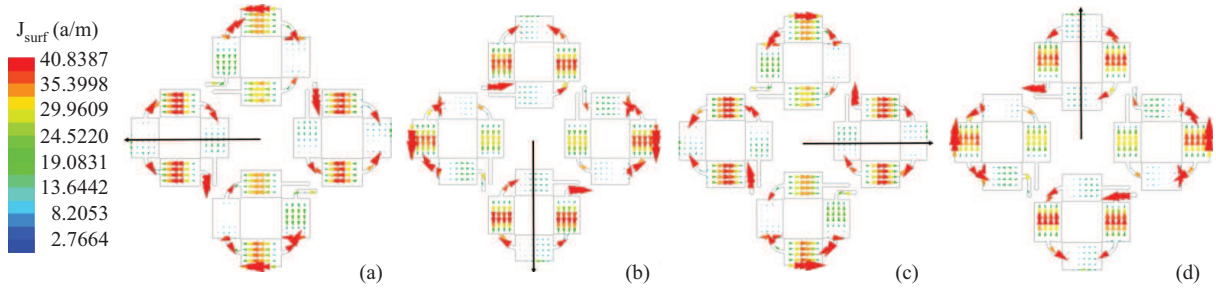

Fig. 7. Surface current distributions on the proposed antenna array in a period at 5.8 GHz: (a) – $t = 0$, (b) – $t = T/4$, (c) – $t = T/2$ and (d) – $t = 3T/4$

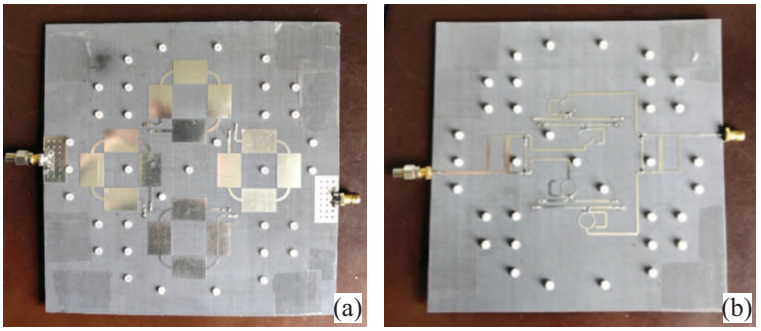

Fig. 8. Photographs of the proposed antenna array: (a) – top view, (b) – back view

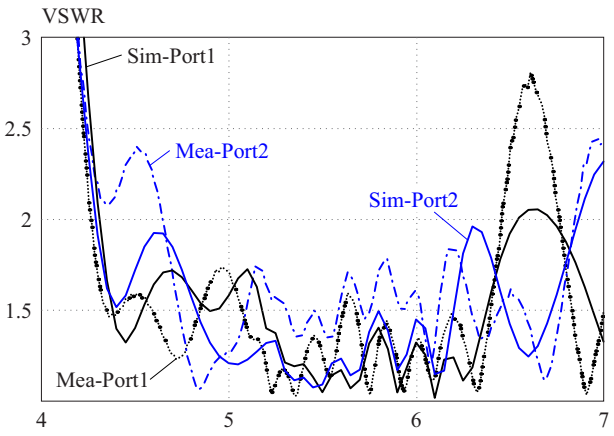

Fig. 9. Measured and simulated VSWR of the studied array

a relatively large gain variation. Figure 3 shows the S parameter of the antenna subarray, indicating an impedance bandwidth of 10 % when referred to $|S_{11}| \leq -10$ dB. Figure 4 is the normalized radiation patterns at different frequencies; it is seen the main beam is deflected against frequency. In order to further enhance the AR bandwidth and impedance bandwidth of the antenna, a 4×4 antenna array is developed.

3 Dual circularly polarized 4×4 array based on the studied subarray

The radiation patches of the traveling wave antenna array based on the 2×2 subarray is shown in Fig. 5(a). The arrangement is rotated in order and each subarray is excited with 90° phase difference. If port 1 is excited, ports A_1, B_1, C_1, and D_1 will be fed under the phases of 0°, 90°, 180°, 270° at the same time. The same is true for exciting port 2. The top and bottom layers are connected by metal posts. Each post has a diameter of

Table 1. Comparisons of some dual-CP antenna (array)

Ref	Elements	Layers	Bandwidth (VSWR < 2)	AR bandwidth (< 3 dB)	Dimension (λ_0)	3 dB gain bandwidth	Beam deflection against frequency
(5)	2×4	2	12.5%/14.7%	12.5%/14.7%	3.4×1.6	> 12%	Yes
(11)	1×7	1	5.5%	9.8%	2.1×2.1	> 9.8%	No
(14)	1×6	3	6.7%	3.77%			No
This work	4×4	2	38%/30.2%	20.7%/22.4%	2.3×2.3	11%/12.7%	No

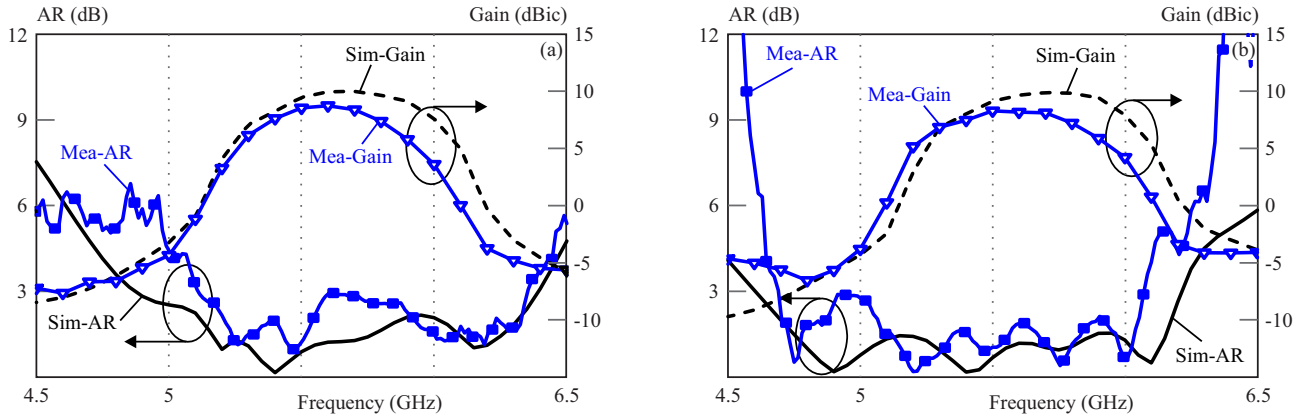

Fig. 10. Measured and simulated AR and attained gain: (a) – port1 and (b) – port2

$SW_1 = 0.5$ mm , and the ground hole has a diameter of $SW_2 = 1.5$ mm . The central spacing between the subarrays is $S = 0.95\,\lambda_0$, where λ_0 is the wavelength at the central frequency of 5.8 GHz in free space.

The feeding structure and cross-sectional view of the antenna array are shown in Fig. 5(b). The feeding structure consists of two wideband baluns and four Wilkinson power dividers. The design of such a wideband balun can be seen in [13], and the simulated results are shown in Fig. 6.

The simulated surface current on the patches at four intervals, namely at $t = 0$, $T/4$, $T/2$ and $3T/4$, is presented in Fig. 7, where T is a period of time. It is clear that at $t = 0$ and $t = T/4$, the main current is along negative y-direction and negative x-direction, while at $t = T/2$ and $3T/4$, the main current is along positive y-direction and positive x-direction. Due to the similar amplitudes of current at both directions and 90° difference between x-direction and y-direction, thus CP radiation is generated. It is worth noting that each patch only generates radiation along x-direction or y-direction, so the proposed antenna is circularly polarized radiation that is linearly synthesized in free space.

4 Experimental characterization of the proposed antenna array

The developed prototype array was fabricated and experimentally characterized for the electromagnetic performance. Figure 8 shows the photograph of the developed 4×4 demonstrator and measurement system. The proposed antenna array was simulated by Ansoft HFSS and measured in standard anechoic chamber. Measured and simulated reflection coefficients of each port are shown in Fig. 9. The simulated impedance bandwidth for VSWR < 2 is 38 %, from 4.3 to 6.5 GHz. The measured impedance bandwidth for VSWR < 2 is 30.2 %, from 4.65 to 6.4 GHz.

Figure 10 shows the measured and simulated AR and realized gain of the antenna array for each port. For port1, the simulated 3-dB AR bandwidth is 26.5 %, from 4.8 to 6.4 GHz, while the measured 3-dB AR bandwidth is 20.7 %, from 5.1 to 6.3 GHz. The measured 3 dB gain bandwidth is 11 %, from 5.3 to 5.9 GHz, and the maximum gain is 8.7 dBi at 5.5 GHz. For port 2, the simulated 3-dB AR bandwidth is 27.5 %, from 4.6 to 6.2 GHz, while the measured 3-dB AR bandwidth is 22.4 %, from 4.7 to 6 GHz. The measured 3 dB gain bandwidth covers 12.7 %, from 5.2 to 5.9 GHz, and the maximum gain is 8.3 dBi at 5.5 GHz. The discrepancies between simulated and measured results could be attributed to the fabrication tolerance of the PCB and the alignment problems of two layers during the assembling process.

The simulated and measured radiation patterns for two ports at 5.5, 5.8 and 6.0 GHz are shown in Figs. 11 and 12, where Fig. 11 is corresponding to port 1 and Fig. 12 is related to port 2. They agree well between the measured data and simulated results. It is worth noting that the back lobe is large; the reason is that the microstrip-line feeding network on the bottom has a cer-

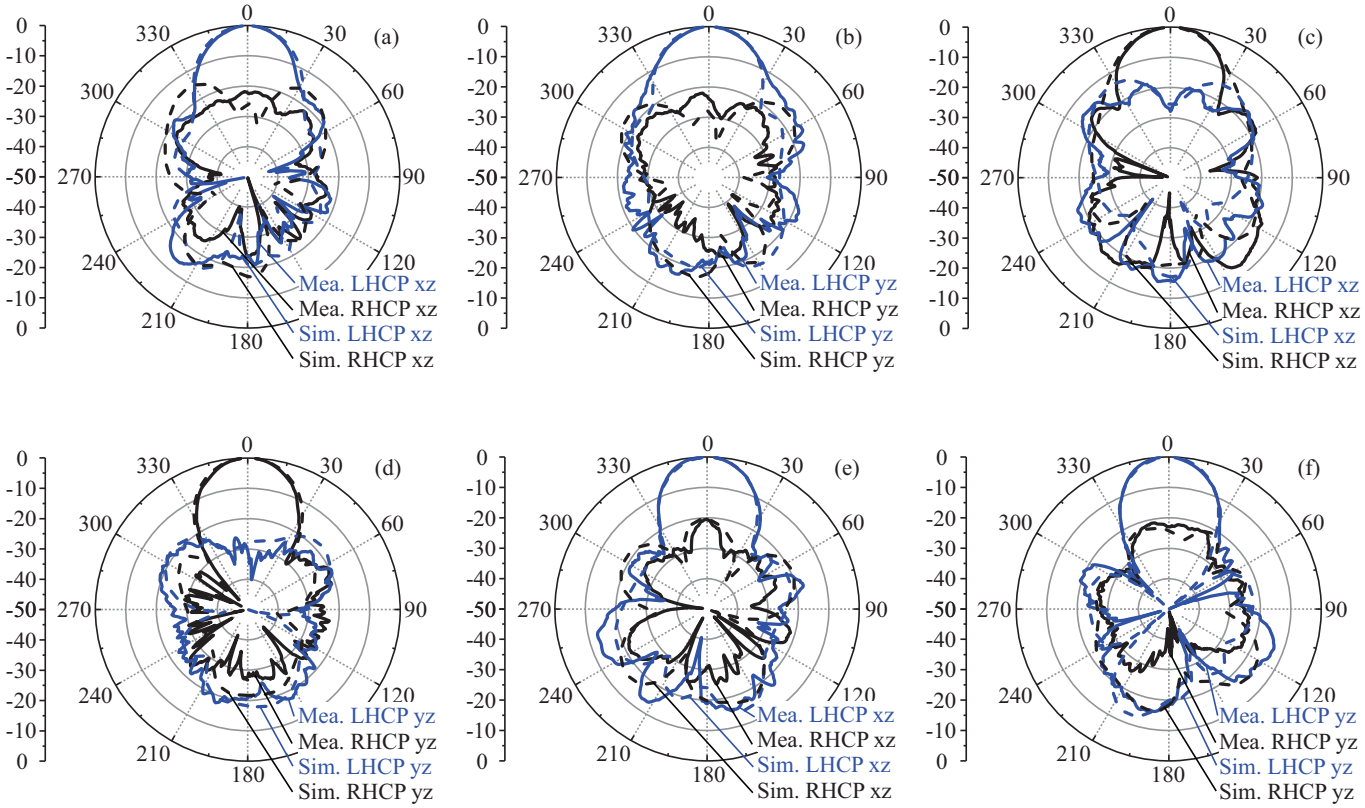

Fig. 11. Measured and simulated radiation patterns at port 1: (a) – xz plane, (b) – yz plane at 5.5 GHz, (c) – xz plane, (d) – yz plane at 5.8 GHz, (e) – xz plane, (f) – yz plane at 6.0 GHz

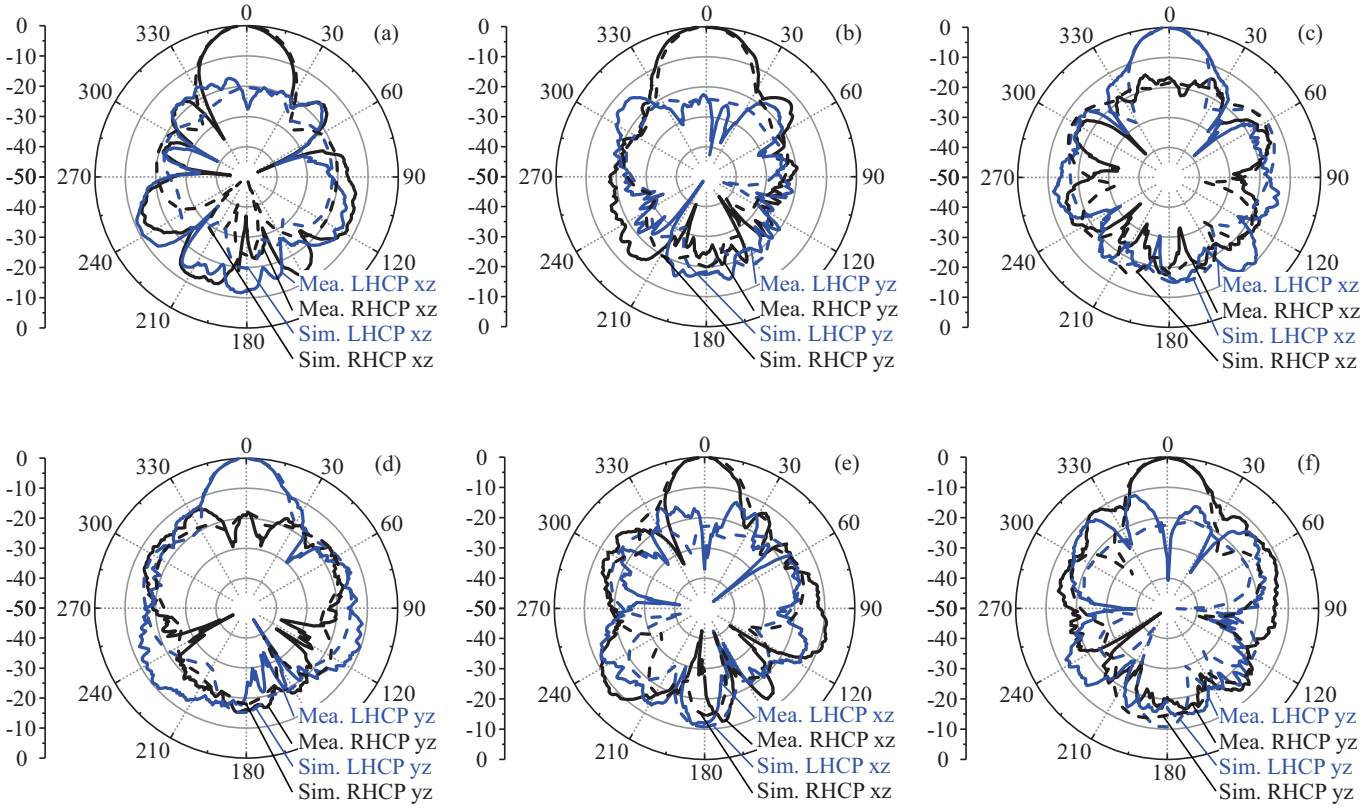

Fig. 12. Measured and simulated radiation patterns at port 2: (a) – xz plane, (b) – yz plane at 5.5 GHz, (c) – xz plane, (d) – yz plane at 5.8 GHz,. (e) – xz plane, (f) – yz plane at 6.0 GHz

tain effect on the radiation. As compared to the subarray, the beam of the array is not deflected against frequency due to the use of sequential rotation to construct the array. The difference in performance of the two ports is due to the asymmetry of the antenna structure.

Further, for performance comparisons, Table 1 shows the performances of the proposed antenna and other dual-CP antennas. The proposed antenna features wide impedance bandwidth and AR bandwidth as compared to other dual-CP antennas. Moreover, due to the symmetry of the radiation structure, the radiation main beam does not change with frequency.

5 Conclusion

A low-cost dual-CP traveling wave antenna based on linearly polarized patch element on microstrip transmission-line is proposed and validated in this paper. The demonstrated 4×4 antenna array can achieve 30 % impedance bandwidth for each port. One of the ports is capable of achieving 20.7 % 3-dB AR bandwidth and 11 % 3 dB gain bandwidth. The other port is capable of achieving 22.4 % 3-dB AR bandwidth and 12.7 % 3-dB gain bandwidth. The developed antenna array implements dual circular polarization with a simple structure and wide operating bandwidth.

Acknowledgements

This work was partly supported by the China Petroleum Logging Company (grant no. CPL-2018A20), and by the State Key Laboratory of Millimeter Waves (Grant no. K202121)

References

[1] Y. Li, Z. Zhang, and Z. Feng, "A sequential-phase feed using a circularly polarized shorted loop structure," *IEEE Transactions on Antennas and Propagation*, vol. 61, no. 3, pp. 1443–1447, Mar 2013.

[2] C. Deng, Y. Li, Z. Zhang, and Z. Feng, "A wideband sequential-phase fed circularly polarized patch array," *IEEE Transactions on Antennas and Propagation*, vol. 62, no. 7, pp. 3890–3893, July 2014.

[3] Q. Zhu, K.-B. Ng, and C.-H. Chan, "Printed circularly polarized spiral antenna array for millimeter-wave applications," *IEEE Transactions on Antennas and Propagation*, vol. 65, no. 2, pp. 636–643, Feb 2017.

[4] K.-H. Lu and T.-N. Chang, "Circularly polarized array antenna with corporate-feed network and series-feed elements," *IEEE Transactions on Antennas and Propagation*, vol. 53, no. 10, pp. 3288–3292, Oct 2005.

[5] Y. Shen, S. Zhou, G. Huang, and T. Chio, "A compact dual circularly polarized microstrip patch array with interlaced sequentially rotated feed," *IEEE Transactions on Antennas and Propagation*, vol. 64, no. 11, pp. 4933–4936, Nov 2016.

[6] R. Xu, J. Li, J. Yang, K. Wei, and Y. Qi, "A design of U-shaped slot antenna with broadband dual circularly polarized radiation," *IEEE Transactions on Antennas and Propagation*, vol. 65, no. 6, pp. 3217–3220, June 2017.

[7] Y. Cai, Y. Zhang, Z. Qian, W. Cao, and S. Shi, "Compact wideband dual circularly polarized substrate integrated waveguide horn antenna," *IEEE Transactions on Antennas and Propagation*, vol. 64, no. 7, pp. 3184–3189, July 2016.

[8] P. Hallbjorner, I. Skarin, K. From, and A. Rydberg, "Circularly polarized traveling-wave array antenna with novel microstrip patch element," *IEEE Antennas and Wireless Propagation Letters*, vol. 6, pp. 572–574, 2007.

[9] Y.-H. Yang, B.-H. Sun, and J.-L. Guo, "A low-cost, single-layer, dual circularly polarized antenna for millimeter-wave applications," *IEEE Antennas and Wireless Propagation Letters*, vol. 18, no. 4, pp. 651–655, Apr 2019.

[10] Y.-H. Yang, J.-L. Guo, B.-H. Sun, Y.-M. Cai, and G.-N. Zhou, "The design of dual circularly polarized series-fed arrays," *IEEE Transactions on Antennas and Propagation*, vol. 67, no. 1, pp. 574–579, Jan 2019.

[11] S.-J. Chen, C. Fumeaux, Y. Monnai, and W. Withayachumnankul, "Dual circularly polarized series-fed microstrip patch array with coplanar proximity coupling," *IEEE Antennas and Wireless Propagation Letters*, vol. 16, pp. 1500–1503, 2017.

[12] J. Huang, "A technique for an array to generate circular polarization with linearly polarized elements," *IEEE Transactions on Antennas and Propagation*, vol. 34, no. 9, pp. 1113–1124, Sep 1986.

[13] C.-G. Sun, J.-L. Li, S.-Y. Yin, and S.-S. Gao, "Broadband branch-line balun with good isolation and impedance matching," *Electromagnetics*, vol. 38, no. 5, pp. 273-282, May 2018.

[14] Q. Luo, S. Gao, M. Sobhy, J. T. S. Sumantyo, J. Li, G. Wei, J. Xu, and C. Wu, "Dual circularly polarized equilateral triangular patch array," *IEEE Transactions on Antennas and Propagation*, vol. 64, no. 6, pp. 2255–2262, June 2016.

Received 24 October 2021